


The Circle-Fit Method Helps Make Reliable Cortical Thickness Measurements Regardless of Humeral Length

Geriatric Orthopaedic Surgery
& Rehabilitation
Volume 9: 1-7
© The Author(s) 2018
Article reuse guidelines:
sagepub.com/journals-permissions
DOI: 10.1177/2151459318818163
journals.sagepub.com/home/gos



Trevor J. Shelton, MD, MS¹ , Amy E. Steele BS², Augustine M. Saiz, MD¹, Kent N. Bachus, PhD^{3,4}, and John G. Skedros, MD^{4,5}

Abstract

Background: Although proximal humerus strength/quality can be assessed using cortical thickness measurements (eg, cortical index), there is no agreement where to make them. Tingart and coworkers used measurements where the proximal endosteum becomes parallel, while Mather and coworkers used measurements where the periosteum becomes parallel. The new circle-fit method (CFM) makes 2 metaphyseal (M1-M2) and 6 diaphyseal (D1-D6) measurements referenced from humeral head diameter (HHD). However, it is unknown whether these locations correlate to humeral length (HL). Accordingly, we asked: (1) Does HHD, Tingart distance, and Mather distance correlate with HL? (2) What is the location of HHD, Tingart distance, and Mather distance as a percentage of HL? and (3) Which CFM D1-D6 locations correlate with Tingart and Mather distances? **Materials and Methods:** Measurements made on cortical thickness (CT) scout views of 19 humeri (ages: 16-73 years) included HHD, distances from the superior aspect of the humerus to proximal Tingart and Mather locations, and HL. **Results:** Intraclass correlation was excellent for CFM-HHD, poor for Tingart, and moderate for Mather. The CFM-HHD had a stronger correlation to HL than Tingart and Mather. Mean HHD was 15.5% (0.9%) of HL while Tingart was 27.0% (4.1%) and Mather was 23.2% (3.8%). Tingart distance corresponded to D2/D3 CFM locations while the Mather distance was similar to D1/D2. **Discussion:** The CFM reliably correlates with HL and provides a stronger correlation and less variance between specimens than the Tingart or Mather Methods. **Conclusions:** Because the CFM produces reliable percent of HL locations, it should be used to define locations for obtaining biomechanically relevant CT measurements such as cortical index. Stronger correlations of these CFM-based measurements with proximal humerus strength will be important for developing advanced algorithms for fracture treatment.

Keywords

humeral head, humeral length, proximal humerus fracture, cortical index, cortical thickness, bone quality, humerus, osteoporosis

Submitted October 10, 2018. Revised November 14, 2018. Accepted November 15, 2018.

Introduction

Proximal humerus fractures are primarily seen in the elderly population following a ground-level fall in large part because they are a true osteoporotic or fragility fracture.¹⁻³ As the percentage of our elderly population increases, it is expected that there will be huge increases in the numbers of adults with osteoporosis although the fracture rate in this demographic appears to have plateaued.⁴ As such, it is important to have metrics that are relatively easy to obtain in clinical and research settings for assessing bone strength/quality to help guide treatment options.

Bone strength and quality are being assessed for clinical and research purposes by making measurements on routine anterior-posterior (AP) radiographs of the proximal humerus.⁵⁻⁸

Cortical index (CI) is the most common measurement employed in clinical settings and is defined as the difference between the outer diameter (OD) and inner diameter (ID)

¹ Department of Orthopaedics, University of California, Davis, Sacramento, CA, USA

² School of Medicine at University of California at Davis, Sacramento, CA, USA

³ Department of Veterans Affairs, Salt Lake City, UT, USA

⁴ Department of Orthopaedics, University of Utah, Salt Lake City, UT, USA

⁵ Utah Orthopaedic Specialists, Salt Lake City, UT, USA

Corresponding Author:

Trevor J. Shelton, Department of Orthopaedics, University of California, Davis, 4860 Y Street, Suite 3800, Sacramento, CA 95817, USA.

Email: tjshelton@ucdavis.edu



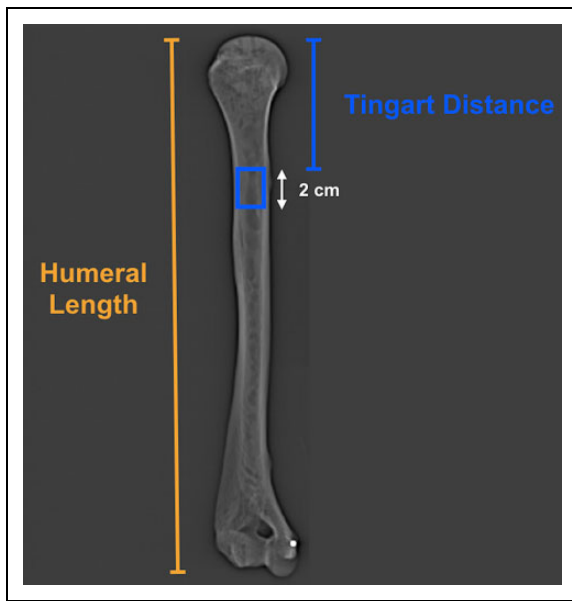


Figure 1. The Tingart method fits a 2-cm tall rectangle to the most proximal level of the humeral diaphysis where the endosteal surfaces of the lateral and medial cortices become parallel.¹³ The distance from the superior aspect of the humeral head to the superior aspect of the rectangle is recorded as the Tingart distance.

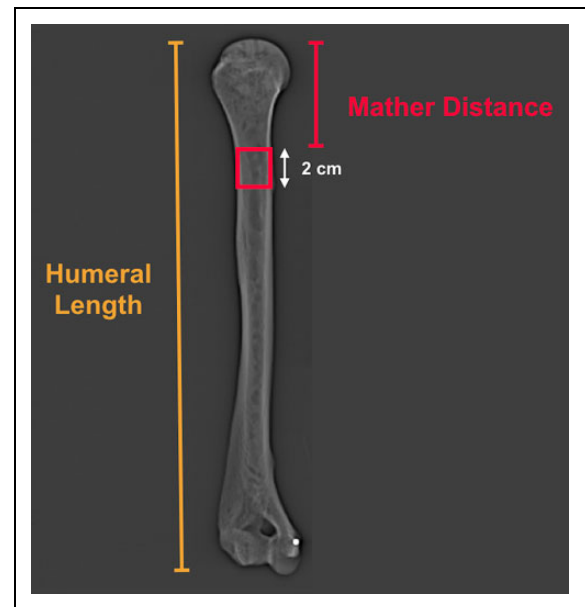


Figure 2. The Mather method fits a 2-cm tall rectangle to the most proximal level of the humeral diaphysis where the periosteal surfaces (outer cortical margins) of the lateral and medial cortices become parallel to each other.¹⁴ The distance from the superior aspect of the humeral head to the superior aspect of the rectangle was then recorded as the Mather distance.

divided by the OD [$CI = (OD - ID)/OD$; lower CI values indicate weaker bone].⁸⁻¹³ Another common measurement is the mean combined cortical thickness (MCCT), which is defined as the OD minus the ID [$MCCT = OD - ID$] and has been shown to have a stronger correlation with bone strength than does CI.^{6,7,11,13,14} Measurements of CI and MCCT are important in clinical settings. For example, these metrics can help surgeons evaluate bone quality/mass in the setting of proximal humerus fractures where measurements can be made on the fractured and nonfractured side, which can help guide surgical decision-making, determine bone quality and mass distribution prior to shoulder arthroplasty, and help quickly determine reduced bone quality and fracture strength of the proximal humerus.^{5-7,9,10,13,15,16} Although there is no agreement as to where measurements of CI and MCCT should be made, it can be agreed upon that these measurements should be made at a reproducible location.^{6-8,13,14,17} One way of ensuring a consistent location would be to identify a landmark that is at a consistent location as a percent of humeral length (HL), allowing locations of measurements to be normalized between patients where humerus size can vary greatly. This would in turn lead to better correlation of CI and MCCT to fracture load.

A common method for making measurements of CI and MCCT was proposed by Tingart et al.¹³ The Tingart method is made by fitting of a 2-cm tall rectangle at the point on the humerus where the endosteal surfaces become parallel (Figure 1). This method can be performed on AP radiographs obtained in clinic but incurs high interobserver (intraclass correlation coefficient [ICC] = 0.35 [0.17, 0.55]) and intraobserver (ICC = 0.22 [0.00, 0.66]) errors due to difficulty

defining parallelism of the endosteal surfaces.^{18,19} A similar method was used by Mather et al except they used a 2-cm tall rectangle fit at the point on the humerus where the periosteal surfaces become parallel (Figure 2).¹⁴ However, like the Tingart method, the Mather method also has a high interobserver (ICC = 0.39 [0.19, 0.59]) and intraobserver (ICC = 0.31 [0.00-0.75]) error.^{18,19}

Recently, a circle-fit method (CFM) has been described where radiographs are used to fit a circle to the periphery of the humeral head in order to establish 2 metaphyseal (M1-M2) and 6 diaphyseal locations (D1-D6) where CI and MCCT can be measured (Figure 3). This method has been shown to incur minimal interobserver variations when compared to the Tingart and Mather methods.^{18,19} However, in these recent studies, only the upper half of the humeri were used. It is currently unknown whether humeral head diameter (HHD) obtained when using the CFM or the locations along the humeral shaft obtained from the Tingart method (“Tingart distance”) or Mather method (“Mather distance”) scales proportionally with HL. Answering this question is a logical next step in this area of research as measurements need to be made consistently and at comparable anatomical locations regardless of differences in bone size. Determining whether these variables scale proportionally with bone length is important because the measurements of CI and MCCT could be made at the same percentage of total HL regardless of the size of the bone, which is an important step in advancing algorithms that guide treatment in proximal humerus fractures.^{8,20,21} Accordingly, we asked: (1) Does HHD (from the CFM), Tingart distance, and

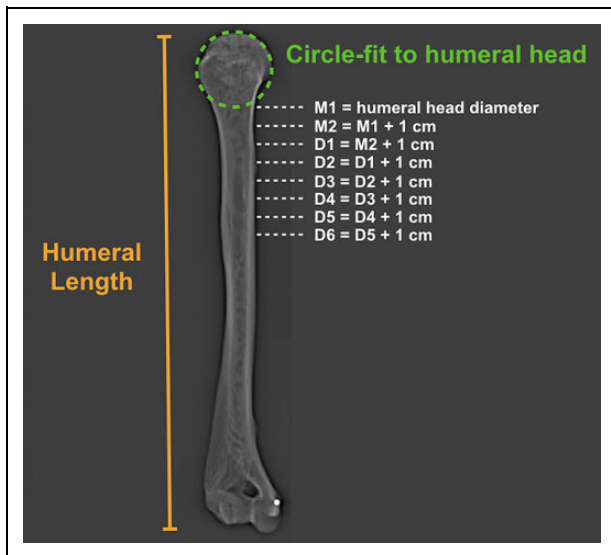


Figure 3. The circle-fit method (CFM) fits a digitized circle to the humeral head and the diameter of the humeral head recorded.¹⁸ The distal-most edge of the circle was defined as M1 (metaphysis = surgical neck region). Seven successive levels or locations were then separated by 1 cm, producing a second metaphyseal level (M2) and 6 diaphyseal levels (D1-D6).

Mather distance correlate with humerus length? (2) And if they do correlate, then what is the location of HHD, Tingart distance, and Mather distance as a percentage of humerus length? (3) Which diaphyseal locations (D1-D6) from the CFM correspond most closely with the Tingart distance and Mather distance?

Materials and Methods

With institutional review board approval, this study used AP scout view localizers taken from full-length 1.25 mm sliced computed tomography (CT) scans from 19 deidentified fresh-frozen cadaveric specimens. A total of 19 humeri (15 left and 4 right humeri, age 37.5 [20.5] years [range: 16-73], 12 men, 7 females, and mean length of 32.0 [2.6] cm) were used. Soft tissues were manually removed from the humeri prior to being CT scanned. As described in previous studies of humeri, steps were taken to standardize the AP projection.^{18,22-24} This was done by placing the humeral head directly on the platform (equivalent to the “cassette” in conventional nondigital imaging) with the long axis of the diaphysis aligned parallel to the platform. Each bone was externally rotated to achieve the true AP plane, which resembles closely the method of Zhang et al.²⁵ The diaphysis was supported with modeling clay to avoid inadvertent rotation.

Images were imported into an open source medical image viewer (Horos, www.horosproject.org) and measurements of HHD using the CFM,¹⁸ distance from superior aspect of humeral head to proximal location of Tingart measurements (Tingart distance),¹³ distance from superior aspect of humeral head to proximal location of the Mather measurements (Mather distance),¹⁴ and overall HL were made.

Circle-Fit Method

An adjustable digitized circle was visually best fit to the periphery of the humeral head, and the diameter of the humeral head was recorded (Figure 3).¹⁸ In accordance with this method, the distal-most edge of the circle was defined as M1 (metaphysis = surgical neck region). Seven successive levels (locations) were then separated by 1 cm, producing a second metaphyseal level (M2) and 6 diaphyseal levels (D1-D6). The HHD was then determined as a percent of HL.

Tingart Method

Using the Tingart method, a 2-cm tall rectangle was fit to the proximal diaphysis at the most proximal level of the humeral diaphysis where the endosteal surfaces of the lateral and medial cortices become parallel to each other (the proximal most edge of the rectangle is placed where parallelism starts).¹³ The distance from the superior aspect of the humeral head to the superior aspect of the rectangle was then recorded as the Tingart distance (Figure 1). This “Tingart distance” was then determined as a percent of HL.

Mather Method

Using the Mather method, a 2-cm tall rectangle was fit to the proximal diaphysis at the most proximal level of the humeral diaphysis where the periosteal surfaces (outer cortical margins) of the lateral and medial cortices become parallel to each other (the proximal most edge of the rectangle is placed where the parallelism starts).¹⁴ The distance from the superior aspect of the humeral head to the superior aspect of the rectangle was then recorded as the Mather distance (Figure 2). This “Mather distance” was then determined as a percent of HL.

Statistical Analysis

Two orthopedic surgery residents and one medical student made the measurements on all 19 specimens independently in order to quantify intraobserver repeatability of the 3 measurements: (1) HHD as a percent of HL, (2) Tingart distance as a percent of HL, and (3) Mather distance as a percent of HL. A single factor analysis of variance with repeated measures computed the ICC for the 3 measurements. The factor was the observer making the measurements with 3 levels (2 orthopedic surgery residents and medical student). An ICC value of >0.75 indicated excellent agreement, 0.5-0.75 moderate agreement, and <0.5 poor agreement.

Mean (standard deviation) was reported for continuous variables (ie, length measurements). Normality of measurements was assessed using a Shapiro-Wilk test. A linear regression computed the Pearson correlation coefficient (r) to determine whether HHD, Tingart distance, or Mather distance correlated with HL. A Kruskal-Wallis test was used with a post hoc Steel-Dwass to determine which diaphyseal locations (D1-D6) determined by the CFM correlated with the Tingart distance and Mather distance. Computations were performed with statistical

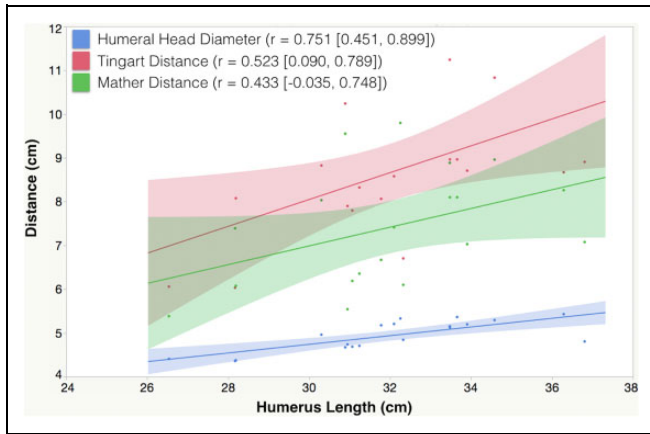


Figure 4. Plot of humeral head diameter (blue), Tingart distance (red), and Mather distance (green) versus humeral length. Dark lines represent the best fit line while shaded areas represent 95% confidence intervals. Humeral head diameter had a better correlation ($r = 0.751$ [0.451, 0.899], [$P < .001$]) compared to the Tingart distance ($r = 0.523$ [0.090, 0.789], [$P = .022$]) and Mather distance ($r = 0.433$ [-0.035, 0.748], [$P = .069$]).

software (JMP, v13.0, <http://www.jmp.com>). Significance was set at $P < .05$.

Results

The mean HL was 32.0 (2.6 cm; range 26.5-36.8 cm). The interobserver reliability was excellent for the HHD as a percent of HL (ICC = 0.876), poor for the Tingart distance as a percent of HL (ICC = 0.396), and poor for the Mather distance as a percent of HL (ICC = 0.474).

For correlations of HHD, Tingart distance, and Mather distance with humerus length, the HHD had the strongest correlation followed by the Tingart and Mather distances. The HHD had a moderate correlation with HL ($r = 0.751$ [0.451, 0.899], [$P < .001$]) while the Tingart distance had a weak correlation ($r = 0.523$ [0.090, 0.789], [$P = .022$]) and very little correlation with the Mather distance ($r = 0.4326$ [-0.035, 0.748], [$P = .069$]; Figure 4). The mean HHD was 4.9 (0.3 cm) or 15.5% (0.9%) of the HL (Figure 5). The mean Tingart distance was 8.7 (1.5 cm) or 27.0% (4.1%) of the HL. The mean Mather distance was 7.4 (1.3 cm) or 23.2% (3.8%) of the HL.

The Tingart distance as a percent of HL was found to correlate with the D2 ($P = .729$) and D3 ($P = .690$) locations of the CFM while the Mather distance as a percent of HL correlates with the D1 ($P = .999$) and D2 ($P = .670$) locations (Table 1). The Tingart distance as a percent of HL also did not differ significantly from the Mather distance as a percent of HL ($P = .130$).

Discussion

Having metrics to assess bone strength and quality is considered important in biomechanical studies of the quality, mass distribution and strength of the proximal humerus, and also for

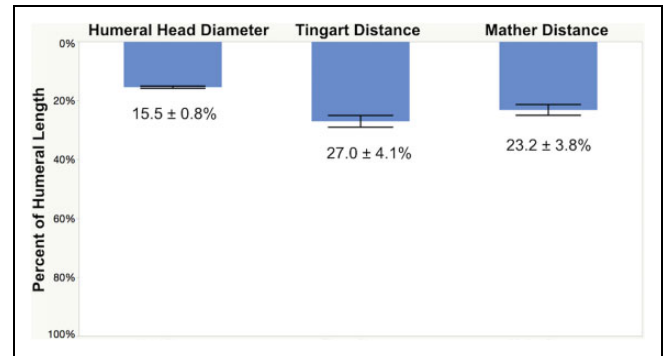


Figure 5. Column plot with 95% confidence intervals of humeral head diameter, Tingart distance, and Mather distance as a percent of humeral length. Means (standard deviations) provided.

Table 1. Metaphyseal and Diaphyseal Locations Determined From the Circle-Fit Method as a Percent of Humeral Length and Relationship to Tingart and Mather Distance.^a

Location	Percent of Humeral Length	P Value Compared to Tingart Distance ^b	P Value Compared to Mather Distance ^b
M1 (humeral head diameter)	15.4% (0.8%)	<.001	<.001
M2 (M1 + 1 cm)	18.6% (1.0%)	<.001	.001
D1 (M2 + 1 cm)	21.8% (1.2%)	.001	.999
D2 (D1 + 1 cm)	24.9% (1.4%)	.729	.670
D3 (D2 + 1 cm)	28.1% (1.6%)	.690	.003
D4 (D3 + 1 cm)	31.2% (1.9%)	.045	<.001
D5 (D4 + 1 cm)	34.3% (2.1%)	<.001	<.001
D6 (D5 + 1 cm)	37.5% (2.4%)	<.001	<.001
Tingart distance	27.0% (4.1%)	–	.130
Mather distance	23.2% (3.8%)	.130	–

^aThe values are presented as mean (standard deviation).

^bThe P values were determined using Kruskal-Wallis test with a post hoc Steel-Dwass. Statistical significance was set at $P < .05$.

clinical purposes including the assessment of bone density/osteoporosis and treatment of proximal humerus fractures.^{5-8,15} However, because current methods of measuring CI and MCCT have poor interobserver reliability, it is unknown if the locations of those measurements can be normalized between patients of different body size. In a prior study from our institution, it could not be determined how closely the CFM-derived metaphyseal and diaphyseal locations correspond to HL because only the upper halves of the humeri were used.^{18,19} The most important findings of the present study are (1) HHD reliably correlates with 15.5% of the humerus length, (2) this has a stronger correlation and therefore substantially less variance between specimens than the Tingart or Mather methods, and (3) diaphyseal locations D2 and D3 correlate most closely to the Tingart location while D1 and D2 correlate most closely to the Mather location.

Previous studies have shown correlation of humeral head dimensions to HL.^{23,26,27} In the discussion section of the study describing the CFM, Mears et al stated that the correlation of

HHD to HL in an article by Auerbach and Ruff was $r = 0.182$. However, this was a misinterpretation of the findings of Auerbach and Ruff, where this correlation was actually comparing asymmetry between left and right bones.^{18,26} In Auerbach and Ruff original work, they did not correlate HHD to HL; however, their database of measurements is available for review of their raw data. Analyzing the data used by Auerbach et al (provided to us by B. Auerbach) from measurements of 2754 humeri throughout the Holocene revealed a correlation of $r = 0.743$ [0.726, 0.759], $P < .001$ for HHD versus HL, which resembles the strength of the correlation found in the present study ($r = 0.751$).²⁶ A second study where 39 cadaveric humeri were examined, Roberts et al reported that the correlation coefficient between HHD and HL is $r = 0.615$.²³ However, when their data in their Figure 3 scatter plot is reanalyzed to determine the P value for the regression (which was not provided in their study), the r value from their data is 0.621 ($P < .001$). (This reanalysis revealed their use of 111 data points even though they reported only using 39 bones.) A third study using 60 fresh cadaver humeri from the Midwestern United States, Robertson et al found a correlation of $r = 0.72$ between humeral head radius and HL.²⁷ Although these studies had similar correlations of HHD to HL, none of them considered relationships of the Tingart and Mather locations to HL.

Knowing that the humeral head scales proportionately to HL can help surgeons restore length following proximal humerus fractures. Preinjury full-length humerus radiographs are not always available in clinical situations to help guide treatment. However, contralateral shoulder or humerus could be used to guide treatment as there is minimal difference between HHDs from contralateral sides.²⁶⁻²⁸ Since the HHD provides a reliable relationship to HL, measurements of CI and MCCT should be made at locations based on the CFM.¹⁸ The stronger correlation and better interobserver reliability of the CFM when compared to the Tingart or Mather methods (ICC = 0.876 for HHD vs 0.396 for Tingart and 0.474 for Mather) supports the conclusion that the CFM will allow clinicians and researchers to more reliably normalize these data between participants.

Our results also showed that the Tingart distance was similar to D2 ($P = .729$) and D3 ($P = .690$) locations of the CFM while the Mather distance was similar to D1 ($P = .999$) and D2 ($P = .670$) locations. These results are biomechanically, and potentially clinically, important when considering the results of prior cadaveric mechanical testing studies of the proximal humerus.^{6,29} These studies examined relationships between ultimate fracture load (UFL) of the proximal humerus (loaded in a ground-level fall configuration) with CI and MCCT made at 8 locations (M1-M2 and D1-D6). They showed that the strongest correlation with UFL with respect to MCCT was at D4 ($r = 0.67$), which does not correspond to either the Tingart or Mather distances measured in the present study. The strongest correlation with CI was at D3 ($r = 0.61$), which only corresponds to the Tingart distance. These prior biomechanical studies also showed large changes in the strengths of correlations of UFL with CI and MCCT when measurement locations were separated by only 2 to 3 cm along the proximal humerus

diaphysis. For example, the correlation of CI with UFL changed from $r = 0.3$ to 0.6 when the measurement was made at 2 locations that were separated by 2 cm. The correlation of MCCT with UFL changed from $r = 0.4$ to 0.7 when the measurements were made at 2 locations separated by 3 cm. In addition to markedly changing the strengths of correlations between CI or MCCI and UFL, there were also instances when the correlation changed from being statistically significant to nonsignificant when the differences in measurement location were on the order of 2 to 3 cm. In contrast to the Tingart and Mather methods, the CFM avoids the problems of misinterpreting correlations of CI and MCCT with UFL because it reduces both intra- and interobserver variations to negligible levels as shown by the present study, which more rigorously confirms the findings of prior studies.^{18,19} Future biomechanical studies using novel or advanced methods (eg, various fall configurations and loading rates) to compare CI and MCCT to fracture load or fracture treatment would likely have more reliable results using the CFM than the methods of Tingart and Mather.

One limitation of the present study is that only 19 specimens were used. However, as mentioned above, the relationship of HHD and HL in the present study is similar to findings in other studies that used substantially larger samples of humeri.^{23,26-28} Consequently, it seems unlikely that performing these measurements on more participants would change the results of the present study. Additional studies that examine racial and sex differences are nevertheless warranted to determine whether there might be unrecognized influences of these factors.^{25,30} A second limitation of the present study is that rotational error was not assessed for the 3 methods. In the present study, careful attention was placed in positioning the humeri for imaging. In the clinical setting, this is much more challenging and may not be possible in the case of fracture. It is possible that small rotations of the humerus could affect the accuracy and reliability of the CFM and Tingart and Mather methods. Although rotational error was not assessed in the present study, contralateral humerus imaging and understanding the scaling of the HHD to HL will allow surgeons to better plan preoperatively and restore anatomic length.

Conclusions

In conclusion, measurements of CI and MCCT should be assessed from locations based on a circle fit to the humeral head as this produces a reliable location of percent of HL across specimens. Future studies should compare CI and MCCT taken at locations distal to the circle-fit diameter of the humeral head as a way to reliably normalize locations of CI and MCCT measurements between specimens. This, in turn, should yield stronger correlations with fracture load, which will help develop advanced algorithms for proximal humerus fracture fixation and arthroplasty.^{8,20,21}

Authors' Note

All authors contributed to research design, acquisition, interpretation of data, and drafting and revising the manuscript. All authors have

read and approved the final submitted manuscript. The study was approved by our ethical committee.


Declaration of Conflicting Interests

The author(s) declared no potential conflicts of interest with respect to the research, authorship, and/or publication of this article.

Funding

The author(s) disclosed receipt of the following financial support for the research, authorship, and/or publication of this article: This work was supported in part by the US Department of Veterans Affairs Rehabilitation Research and Development Service under Merit Review Awards #I01RX001246.

ORCID iD

Trevor J. Shelton, MD, MS  <https://orcid.org/0000-0002-2032-3371>

References

- Jo MJ, Gardner MJ. Proximal humerus fractures. *Curr Rev Musculoskelet Med.* 2012;5(3):192-198.
- Karl JW, Olson PR, Rosenwasser MP. The epidemiology of upper extremity fractures in the United States, 2009. *J Orthop Trauma.* 2015;29(8):e242-e244.
- Launonen AP, Lepola V, Saranko A, Flinkkila T, Laitinen M, Mattila VM. Epidemiology of proximal humerus fractures. *Arch Osteoporos.* 2015;10:209.
- Kannus P, Niemi S, Sievanen H, Parkkari J. Stabilized incidence in proximal humeral fractures of elderly women: nationwide statistics from Finland in 1970–2015. *J Gerontol A Biol Sci Med Sci.* 2017;72(10):1390-1393.
- Nho SJ, Brophy RH, Barker JU, Cornell CN, MacGillivray JD. Innovations in the management of displaced proximal humerus fractures. *J Am Acad Orthop Surg.* 2007;15(1):12-26.
- Skedros JG, Knight AN, Pitts TC, O'Rourke PJ, Burkhead WZ. Radiographic morphometry and densitometry predict strength of cadaveric proximal humeri more reliably than age and DXA scan density. *J Orthop Res.* 2016;34(2):331-341.
- Skedros JG, Mears CS, Burkhead WZ. Ultimate fracture load of cadaver proximal humeri correlates more strongly with mean combined cortical thickness than with areal cortical index, DEXA density, or canal-to-calcar ratio. *Bone Joint Res.* 2017;6(1):1-7.
- Spross C, Kaestle N, Benninger E, et al. Deltoid tuberosity index: a simple radiographic tool to assess local bone quality in proximal humerus fractures. *Clin Orthop Relat Res.* 2015;473(9):3038-3045.
- Giannotti S, Bottai V, Dell'osso G, et al. Indices of risk assessment of fracture of the proximal humerus. *Clin Cases Miner Bone Metab.* 2012;9(1):37-39.
- Hepp P, Theopold J, Osterhoff G, Marquass B, Voigt C, Josten C. Bone quality measured by the radiogrammetric parameter "cortical index" and reoperations after locking plate osteosynthesis in patients sustaining proximal humerus fractures. *Arch Orthop Trauma Surg.* 2009;129(9):1251-1259.
- Namdari S, Voleti PB, Mehta S. Evaluation of the osteoporotic proximal humeral fracture and strategies for structural augmentation during surgical treatment. *J Shoulder Elbow Surg.* 2012;21(12):1787-1795.
- Osterhoff G, Diederichs G, Tami A, Theopold J, Josten C, Hepp P. Influence of trabecular microstructure and cortical index on the complexity of proximal humeral fractures. *Arch Orthop Trauma Surg.* 2012;132(4):509-515.
- Tingart MJ, Apreleva M, von Stechow D, Zurakowski D, Warner JJ. The cortical thickness of the proximal humeral diaphysis predicts bone mineral density of the proximal humerus. *J Bone Joint Surg Br.* 2003;85(4):611-617.
- Mather J, MacDermid JC, Faber KJ, Athwal GS. Proximal humerus cortical bone thickness correlates with bone mineral density and can clinically rule out osteoporosis. *J Shoulder Elbow Surg.* 2013;22(6):732-738.
- Nho SJ, Brophy RH, Barker JU, Cornell CN, MacGillivray JD. Management of proximal humeral fractures based on current literature. *J Bone Joint Surg Am.* 2007;89(suppl 3):44-58.
- Patterson J, Rungprai C, Den Hartog T, et al. Cortical bone thickness of the distal part of the tibia predicts bone mineral density. *J Bone Joint Surg Am.* 2016;98(9):751-760.
- Tingart MJ, Lehtinen J, Zurakowski D, Warner JJ, Apreleva M. Proximal humeral fractures: regional differences in bone mineral density of the humeral head affect the fixation strength of cancellous screws. *J Shoulder Elbow Surg.* 2006;15(5):620-624.
- Mears CS, Langston TD, Phippen CM, Burkhead WZ, Skedros JG. Humeral head circle-fit method greatly increases reliability and accuracy when measuring anterior-posterior radiographs of the proximal humerus. *J Orthop Res.* 2017;35(10):2313-2322.
- Skedros JG, Mears CS, Langston TD, Phippen CM, Burkhead WZ, Stoddard G. Reply: the humeral head circle-fit method greatly increases reliability and accuracy when measuring anterior-posterior radiographs. *J Orthop Res.* 2017;35(9):1866-1867.
- Carbone S, Mezzoprete R, Papalia M, Arceri V, Carbone A, Gumina S. Radiographic patterns of osteoporotic proximal humerus fractures. *Eur J Radiol.* 2018;100:43-48.
- Mazzucchelli RA, Jenny K, Zdravkovic V, Erhardt JB, Jost B, Spross C. The influence of local bone quality on fracture pattern in proximal humerus fractures. *Injury.* 2017;49(2):359-363.
- Boileau P, Walch G. The three-dimensional geometry of the proximal humerus. Implications for surgical technique and prosthetic design. *J Bone Joint Surg Br.* 1997;79(5):857-865.
- Roberts SN, Foley AP, Swallow HM, Wallace WA, Coughlan DP. The geometry of the humeral head and the design of prostheses. *J Bone Joint Surg Br.* 1991;73(4):647-650.
- Tillett E, Smith M, Fulcher M, Shanklin J. Anatomic determination of humeral head retroversion: the relationship of the central axis of the humeral head to the bicipital groove. *J Shoulder Elbow Surg.* 1993;2(5):255-256.
- Zhang Q, Shi LL, Ravella KC, et al. Distinct proximal humeral geometry in chinese population and clinical relevance. *J Bone Joint Surg Am.* 2016;98(24):2071-2081.
- Auerbach BM, Ruff CB. Limb bone bilateral asymmetry: variability and commonality among modern humans. *J Hum Evol.* 2006;50(2):203-218.

27. Robertson DD, Yuan J, Bigliani LU, Flatow EL, Yamaguchi K. Three-dimensional analysis of the proximal part of the humerus: relevance to arthroplasty. *J Bone Joint Surg Am.* 2000;82-A(11): 1594-1602.
28. Auerbach BM, Ruff CB. Human body mass estimation: a comparison of “morphometric” and “mechanical” methods. *Am J Phys Anthropol.* 2004;125(4):331-342.
29. Langston TD, Mears CS, Phippen CM, Brady ST, Skedros JG. *Inter-Observer Variations When Using Popular Methods to Obtain Cortical Index and Mean Combined Cortical Thickness in Proximal Humerus Radiographs Can Result in Highly Variable Correlations with Fracture Strength.* Orlando, FL: Orthopaedic Research Society; 2016.
30. Aroonjarattham P, Jiamwatthanachai P, Mahaisavariya B, Kiatiwat T, Aroonjaratthammd K, Sittiseripratip K. Three-dimensional morphometric study of the Thai proximal humerus: cadaveric study. *J Med Assoc Thai.* 2009;92(9): 1191-1197.